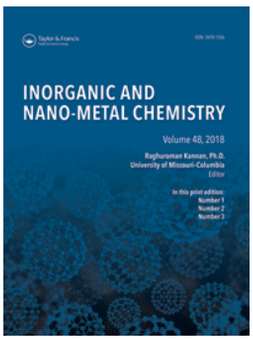

Taylor & Francis
Taylor & Francis Group

Inorganic and Nano-Metal Chemistry

ISSN: 2470-1556 (Print) 2470-1564 (Online) Journal homepage: https://www.tandfonline.com/loi/lsrt21

Folic acid functionalized PEG coated magnetic nanoparticles for targeting anti-cancer drug delivery: Preparation, characterization and cytotoxicity on Doxorubicin, Zoledronic acid and Paclitaxel resistant MCF-7 breast cancer cell lines

Tugba Keskin, Serap Yalcin & Ufuk Gunduz

To cite this article: Tugba Keskin, Serap Yalcin & Ufuk Gunduz (2018) Folic acid functionalized PEG coated magnetic nanoparticles for targeting anti-cancer drug delivery: Preparation, characterization and cytotoxicity on Doxorubicin, Zoledronic acid and Paclitaxel resistant MCF-7 breast cancer cell lines, Inorganic and Nano-Metal Chemistry, 48:2, 150-159, DOI: 10.1080/24701556.2018.1453840

To link to this article: https://doi.org/10.1080/24701556.2018.1453840

INORGANIC AND NANO-METAL CHEMISTRY
2018, VOL. 48, NO. 2, 150–159
https://doi.org/10.1080/24701556.2018.1453840

Taylor & Francis
Taylor & Francis Group

Folic acid functionalized PEG coated magnetic nanoparticles for targeting anti-cancer drug delivery: Preparation, characterization and cytotoxicity on Doxorubicin, Zoledronic acid and Paclitaxel resistant MCF-7 breast cancer cell lines

Tugba Keskin[a], Serap Yalcin[b], and Ufuk Gunduz[a,c]

[a]Middle East Technical University, Department of Biology, Ankara, Turkey; [b]Ahi Evran University, Department of Molecular Biology and Genetics, Kırsehir, Turkey; [c]Middle East Technical University, Department of Biotechnology, Ankara, Turkey

ABSTRACT

In this study, MNPs were synthesized, coated with biocompatible polyethylene glycol (PEG) and conjugated with folic acid. Crystal and chemical structures, shape, size and magnetic properties of synthesized nanoparticles were characterized. Agglomeration tendency of naked nanoparticles were prevented by oleic acid addition during the synthesis. All synthesized MNPs have been found to exhibit superparamagnetic behavior at 23°C and 37°C. Cytotoxic effects of MNPs were investigated on Doxorubicin, Zoledronic acid and Paclitaxel resistant MCF-7 breast cancer cell lines. The synthesized nanoparticles have been found to be suitable for drug targeting in terms of size, shape, magnetic and cytotoxic properties.

ARTICLE HISTORY
Received 2 June 2016
Accepted 14 March 2018

KEYWORDS
Folic acid; Polyethylene glycol (PEG); magnetic nanoparticle; Drug delivery; MCF-7; drug targeting

Introduction

General structure of magnetic nanoparticles (MNPs) is composed of an inner magnetic core which is usually a magnetite (Fe_3O_4) or maghemite (Fe_2O_3) and outer polymeric shell. Magnetic nanoparticles can be targeted to tumor site in the presence of a magnetic field. The polymeric shell renders MNPs biocompatible, prevents their agglomeration and functions as drug reservoir.[1] Different types of polymers and molecules are used for covering surfaces of naked magnetic nanoparticles to stabilize them and for further biological applications. Starch, dextran, polyethylene glycol, fatty acids, polyvinyl alcohol, polyacrylic acid, poly lactides, poly-hydroxybutyrate, gelatin and chitosan are some of the examples of widely used coating material with different purposes.[2–5] PEG is one of the frequently used synthetic polymers to cover MNPs. It gives MNPs a hydrophilic surface and minimizes their agglomeration. Thus, PEG coating enhances the circulation time of MNPs by reducing their phagocytosis by macrophages.[6] According to the aim of the use, unique targeting agents can be tailored to surface of MNPs. Transferrin, lactoferin, elastin, albumin, Tat peptide, RGD peptide and folic acid are remarkable targeting ligands which are able to target cell surface receptors.[2] Folic acid receptors (FR) are found to be overexpressed on different types of cancer cells such as ovarian, brain, kidney, lung, head and neck, breast and colorectal cancers.[7]Normal cells do not express FR or it locates on apical surface of polarized epithelia where drugs cannot reach.[8]Besides, while only reduced folate can be transported in healthy cells, cancer cells are able to transport folate conjugates by FR via receptor mediated endocytosis. In this process, after folic acid ligand of targeting agents binds to FR on cell surface, they are internalized into an endosome. The release of the cargo in nanoparticles becomes easier as pH value decreases in the endosome resulting in entry of drug into cytoplasm. By this mechanism, folic acid covered nanoparticles can overcome drug resistance caused by P-glycoprotein efflux pumps.[9]Folate ligands are not expensive, toxic or immunogenic. Also they can be easily attached to drug carriers and bind to FR with high affinity. They keep their stable form in storage and in circulation for long time.[7]These natural characteristics of folic acid and folic acid receptors on cancer cells make them very efficient agents for drug targeting, immunotherapy and tumor imaging.[8]Since cancer cells overexpress FR, folic acid conjugated agents are primarily taken up into cancer cells, and they can prevent the severe side effects of free drugs and, in addition they may overcome the drug resistance problem.

The aim of this study is synthesis, and characterization of folic acid conjugated, PEG coated magnetic nanoparticles and to indicate their potential as anti-cancer drug targeting system. Here, drug targeting would be by physical effects due to magnetic properties, and by chemical effects due to folic acid conjugation. These nanoparticles may bypass the drug resistance mechanisms which develop during chemotherapy.

Experimentals

Materials

Iron (II) chloride tetrahydrate ($FeCl_2.4H_2O$), iron (III) chloride hexahydrate ($FeCl_3.6H_2O$), oleic Acid, polyethylene monooleate, folic acid, dicyclohexyl carbodiimide (DCC) and

CONTACT Serap Yalcin syalcin@ahievran.edu.tr Department of Molecular Biology and Genetics, Ahi Evran University, Kırsehir, 40100 Turkey; Ufuk Gunduz ufukg@metu.edu.tr Department of Biotechnology, 06800, Middle East Technical University, Ankara, Turkey.

Color versions of one or more of the figures in the article can be found online at www.tandfonline.com/lsrt.

dimethylsulfoxide (DMSO) were purchased from Sigma-Aldrich (U.S.A). Ammonium hydroxide solution (NH_4OH) was obtained from Merck (Germany). Dimethylsulfoxide (cell culture grade) was obtained from Applichem (Germany). MCF-7 monolayer type human epithelial breast adenocarcinoma cell line was provided from Food and Mouth Diseases Institute (Ankara). 1 μM Doxorubicin, 400 nM paclitaxel and 8 μM zoledronic acid resistant cell lines, namely; MCF-7/Dox, MCF-7/Pac and MCF-7/Zol were previously developed from MCF-7 (MCF-7/S) in our laboratory by continuous application of drugs (Demirel et al. 2007). RPMI 1640 medium ((1x), 2.0 g/l $NaHCO_3$ stable glutamine), fetal bovine serum (tested for mycoplasma) were obtained from Biochrom Ag. (Germany). Trypsin-EDTA solution (0.25% Trypsin&EDTA), gentamycin sulphate (50 mg/ml as base), tryphan blue solution (0.5%), cell proliferation kit (XTT assay) were obtained from Biological Industries, Kibbutz Beit Haemek (Israel).

Preparation of magnetic nanoparticles

Magnetic iron oxide (Fe_3O_4) nanoparticles were synthesized for comparison purpose by the coprecipitation of Fe (II) and Fe (III) salts at 1:2 ratio in 150 ml deionized water within a five-necked glass balloon.[10–11]Glass balloon is placed on a heating mantle and stirred by a glass rod of mechanical stirrer, which is inserted into the middle neck of the balloon. It is vigorously stirred in the presence of nitrogen (N_2) gas at 90 ^{0}C. The nitrogen gas prevents oxidation. Ammonium hydroxide (NH_4OH) is added to the system dropwise. The process ends by washing with deionized H_2O until the solution pH is 9.0. For the optimization of synthesis step, three different synthesis experiments were performed. In two of them, 25 ml and 35 ml ammonium hydroxide were used. Speed of perilstaltic pump was adjusted to 0.2. Those nanoparticles were named as N-MNP-1 and N-MNP-2 respectively. In the third experimental setup, 25 ml ammonium hydroxide was added in to system in a shorter time and yield of the sample was labeled as N-MNP-3.

Preparation of oleic acid coated magnetic nanoparticles

Oleic acid was used as surfactant to prevent agglomeration. Oleic acid coated MNPs were synthesized in two different methods. In the first method, after MNP were synthesized and washed, oleic acid was added on MNP solution and stirred for 1 hour by mechanical stirrer.[12] Particles were washed 3 times with ethanol to get rid of excess amount of oleic acid and labeled as OA-MNP-1. In second way, oleic acid was directly added into synthesis system. After black precipitate was obtained, temperature was decreased to 80°C and oleic acid was added into system. Stirring was continued for 24 hours.[11] Sample was labeled as OA-MNP-2.

Functionalization of magnetic nanoparticles with polyethylene glycol

PEG coated MNPs were prepared by two different methods. PEG-MNP-1 nanoparticles were synthesized by mixing OA-MNP-1 with PEG monooleate in aqueous environment for 24 hr. In second method, after the synthesis of oleic acid coated MNP, the temperature of the system was decreased to room temperature, and the aqueous solution of PEG monooleate was added to system and the stirring was continued for an additional 24 h at room temperature. PEG coated MNPs obtained by this method was labeled as PEG-MNP-2. In the synthesis of PEG-MNP-3, after washing OA-MNP-2 with ethanol, they were mixed with aqueous solution of PEG monooleate for 24 hr.

Modification of magnetic nanoparticles with folic acid

Folic acid needs the activation of its carboxyl group with dicyclohexyl carbodiimide (DCC) to conjugate to surface polymer.[13]Folic acid and DCC with 1:1 ratio were added in dimethyl sulfoxide (DMSO) and stirred for 2 h. PEG-MNP-2 sample was added into system and continuously stirred for either 2 h or 24 h under a nitrogen atmosphere. After washing of the nanoparticles with dH_2O, they were freeze-dried for one night. The sample stirred for 2 hr or 24 h labeled as FA-MNP-1 and FA-MNP-2, respectively.

Cell proliferation assay with XTT reagent

The cytotoxic effect of synthesized MNPs on both drug sensitive and drug resistant MCF-7 cells were performed by XTT Cell Proliferation Assay. Drug resistant MCF-7 cell lines are MCF-7/Dox (1000 nM Doxorubicine resistant), MCF-7/Pac (400 nM Paclitaxel resistant) and MCF-7/Zol (8μM Zoledronic Acid resistant). Cells were seeded to 96-well microliter plates (Greiner) at a concentration of 5.0 × 104 cells/well and incubated for 72 h in medium containing horizontal dilutions of drugs. In each plate assay was performed with a column of blank medium control and a cell control columns. Then, XTT reagent (XTT Cell Proliferation Assay, Isreal) was added and soluble product was measured at 500 nm with a Spectromax 340 96-well plate reader (Molecular Devices, USA).

Light microscopy observation of MNP treated cells

To investigate and observe the response of cells to nanoparticles in in vitro conditions, MCF-7/S cells were seeded in 6 well plate (25,000 cell/well) and incubated with 500 μg/ml of N-MNP-1, PEG-MNP-2 and FA-MNP-1. After 48 hr of incubation, cells were observed under light microscopy and images were taken.

Statistical analysis

All data representative of three independent experiments, each run in triplicates and expressed as mean standart error of means (SEM). One-way ANOVA, two-way ANOVA, Tukey and Bonferroni post tests were carried out.

Results and discussion

Transmission electron microscopy (TEM) of MNPs

Shapes and sizes of naked, oleic acid, PEG coated and folic acid functionalized nanoparticles were analyzed by TEM. In Fig. 1, TEM images of N-MNP-1, N-MNP-2 and N-MNP-3, samples

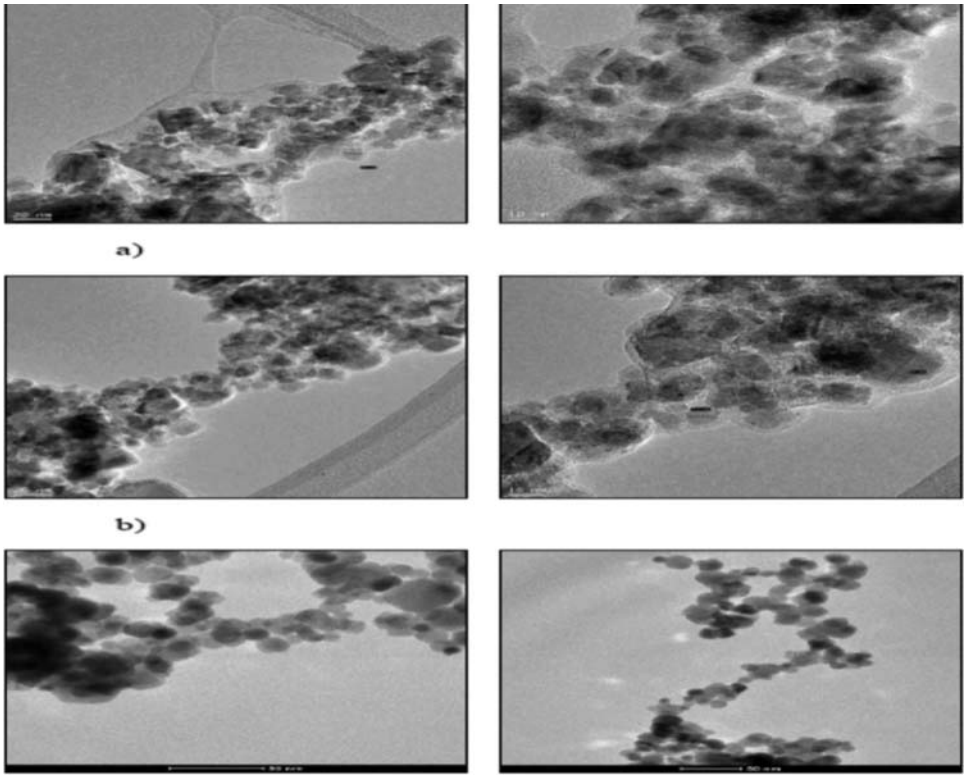

Figure 1. TEM images of N-MNP-1(a), N-MNP-2(b) and N-MNP-3(c).

are shown. Sizes of naked magnetic nanoparticles seemed to be approximately between 10 to 60 nm.

When images of N-MNP-1 and N-MNP-2 samples were compared, particle sizes were found to be similar. TEM image of N-MNP-3 sample exhibited more spherical nanoparticles with similar morphologies compared to N-MNP-1 and N-MNP-2 particles. The yield is high in co-precipitation method; however, synthesized particles usually have broad size distribution between 10–50 nm.[2] In this method, during synthesis pH is important and has a role on particle size and morphology.[1]During synthesis of N-MNP-1 and N-MNP-2 samples, addition of ammonium hydroxide solution to system took 3 to 4 hours by a peristaltic pump. Within this time period, pH of the system was continuously increased and led to precipitation reaction at different pH values. Increase in pH during the reaction may lead to synthesis of particles with irregular morphologies and broad size distribution. On the other hand, during the synthesis of N-MNP-3 particles, ammonium hydroxide solution was given into system in 15 minutes at a higher speed. Hence, pH value of the system increased and fixed in a shorter time. This may cause the reaction to take place in a narrower pH range which probably resulted in narrower size distribution and similar morphologies.

Figure 2a displays TEM images of OA-MNP-1. Size distribution of OA-MNP-1 was found to be between 10–60 nm. Fig. 2b displays TEM images of OA-MNP-2 where sizes of MNPs were found approximately between 10–15 nm. When Fig. 2a and 2b are examined, it is observed that particles of OA-MNP-1 sample were tend to agglomerate more compared to OA-MNP-2 particles. This could be explained by interaction of oleic acid with the surface of nanoparticles. MNPs have Fe-OH hydroxyl groups on their surfaces. Oleic acid interacts with the surface of naked MNP by its –COOH carboxyl group.[14]When oleic acid was added during synthesis, pH of the system was basic since there was still ammonium hydroxide in the system. Interaction between Fe-OH hydroxyl groups of naked MNP and –COOH carboxyl group of oleic acid is easier at high pHs. When oleic acid was added after synthesis, naked MNPs were washed before oleic acid addition until pH 8. After washing, oleic acid and MNPs were mixed at room temperature. Both low pH and higher temperature (80 °C) could affect the interaction of oleic acid with the surfaces of naked MNP. Poor coating of oleic acid layer in OA-MNP-1 sample may result in higher agglomeration. Meanwhile, shapes of OA-MNP-2 nanoparticles are more regular compared to OA-MNP-1 nanoparticles. The naked MNPs which were used in OA-MNP-1 synthesis were belonging to N-MNP-2 samples which have irregular shapes and broad size distribution. In the literature similar results have been reported. Yan et al. synthesized oleic acid coated Fe_3O_4 nanoparticles and added oleic acid after synthesis of particles.[12] In their study agglomeration tendency of oleic acid coated nanoparticles was observed. On the other hand, Liu et al. prepared oleic acid coated nanoparticles by addition of oleic acid to system during the synthesis. Their oleic acid coated Fe_3O_4 particles seemed to prevent agglomeration.[10]

Polyethylene glycol coated nanoparticles were synthesized by three different methods and labeled as PEG-MNP-1, PEG-MNP-2 and PEG-MNP-3. During preparation of PEG-MNP-1 nanoparticles, PEG was not added into system during synthesis. Firstly, naked MNPs were synthesized and washed. After they were coated with oleic acid, PEG coating step was performed. PEG-MNP-2 nanoparticles were synthesized by in situ addition of both oleic acid and PEG during synthesis. PEG-MNP-3 nanoparticles were coated with PEG after washing of oleic acid coated MNP which were synthesized by in situ addition of oleic acid. TEM image of PEG-MNP-2 are given in Fig. 3. PEG-

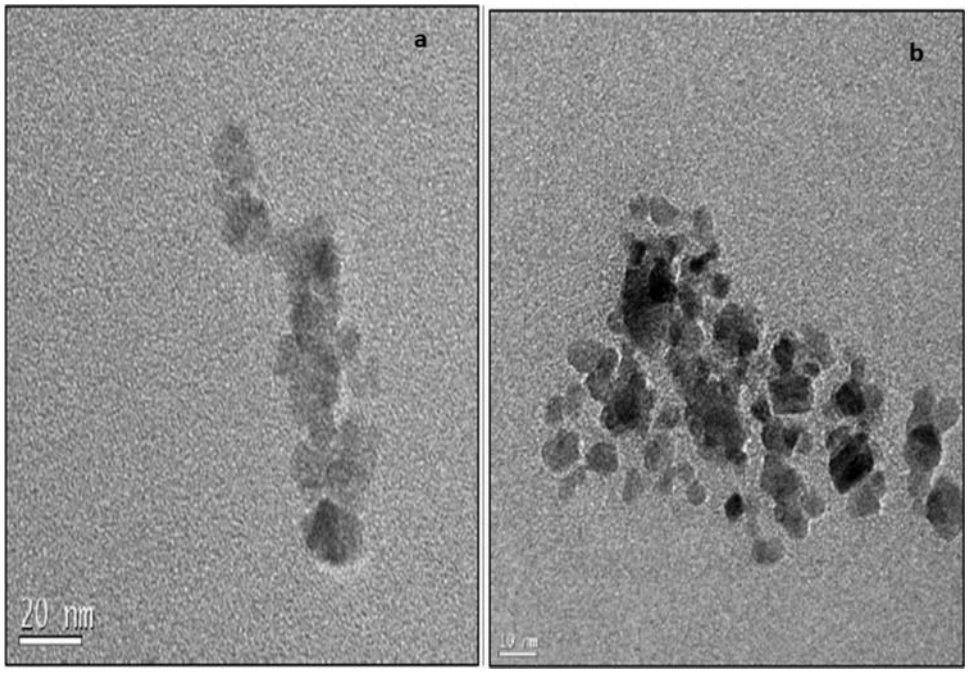

Figure 2. TEM images of OA-MNP-1(a), OA-MNP-2(b).

MNP-1 samples tend to agglomerate and their morphology was irregular with a broad size distribution (data not shown). In Fig. 3, shape and morphology of PEG-MNP-2 nanoparticles are seen more regular and spherical. Their size distribution seemed to be narrower. Their sizes were found to be around 10 nm according to TEM examination. PEG-MNP-2 nanoparticles did not make clusters as much as naked MNP. They seemed agglomerate less compared to PEG-MNP-1 nanoparticles. PEG-MNP-3 nanoparticles were spherical in shape and sized between approximately 10 to 40 nm. Agglomeration of nanoparticles seemed to be prevented better compared to naked nanoparticles (data not shown).

Folic acid can be used as targeting agent in biomedical applications of cancer therapies.[15] In this study, magnetic nanoparticles were functionalized with folic acid after covering with PEG. During folic acid functionalization, reaction time was one of the parameters. Conjugation of folic acid to surface of PEG coated MNP was performed either for 2 hr or for 24 hr and the yields were labeled as FA-MNP-1 and FA-MNP-2, respectively. TEM images of FA-MNP-1 and FA-MNP-2 samples are given in Fig. 4 and 5. Shape and morphology of FA-MNP-1 and FA-MNP-2 nanoparticles were similar. The sizes were between 10–40 nm approximately. They exhibited some degree of agglomeration.

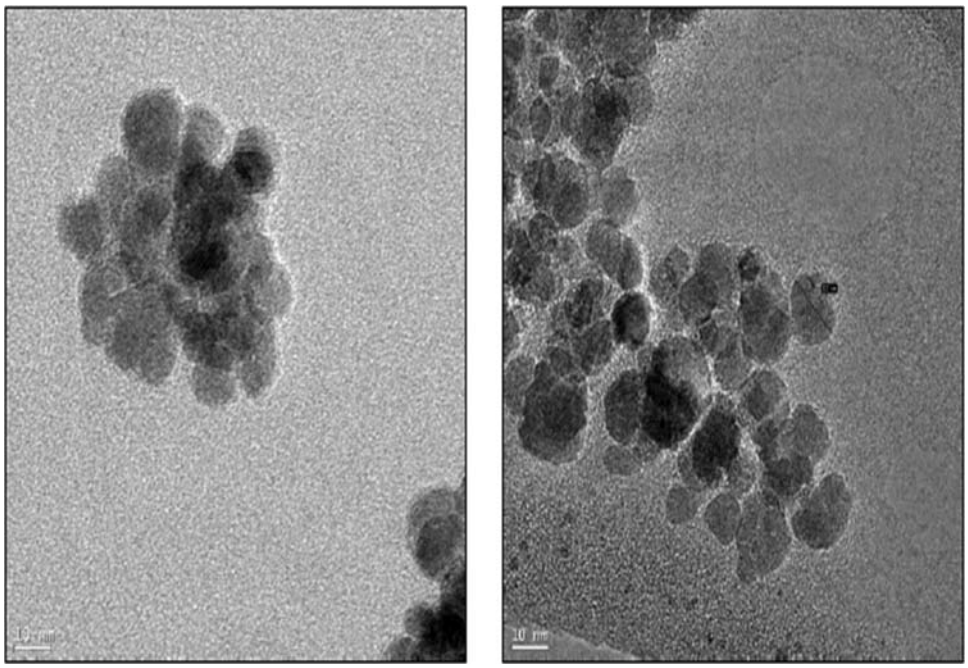

Figure 3. TEM images of PEG-MNP-2.

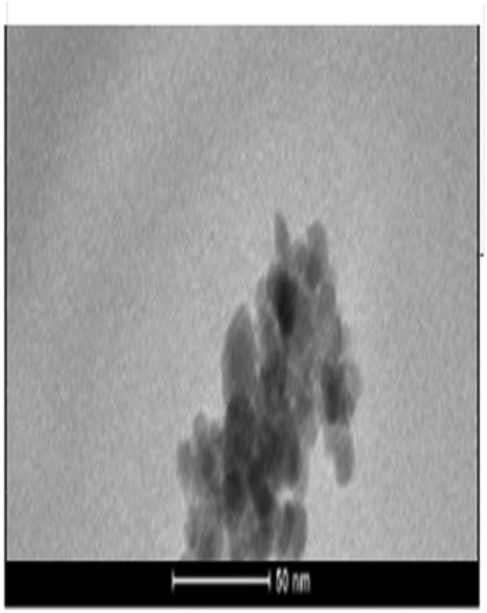

Figure 4. TEM image of FA-MNP-1.

X-ray diffraction (XRD)

Naked MNP, oleic acid coated MNP and PEG coated MNP were analyzed with XRD to identify their crystal structure. Fig. 6 shows XRD patterns of N-MNP-1, N-MNP-2 and N-MNP-3. XRD patterns of all synthesized naked MNP were examined by comparing to peaks of standard magnetite in JCPDS file (PDF no: 01-071-6337).

Standard Fe_3O_4 gives major peaks at 30.22, 35.60, 43.27, 53.68, 57.23, 62.85 2θ (degrees) which are corresponding to specific diffractive plane indexes (220), (311), (400), (422), (511), (440), respectively. N-MNP-1, N-MNP-2 and N-MNP-3 nanoparticles had exactly same peaks with standard magnetite which indicates that all synthesized naked nanoparticle samples

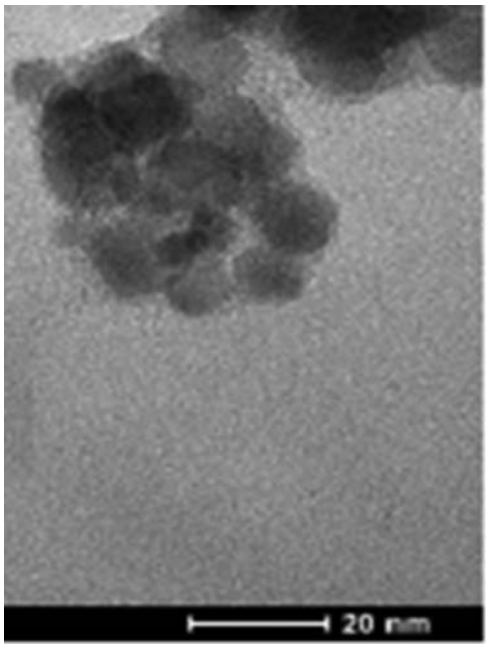

Figure 5. TEM image of FA-MNP-2.

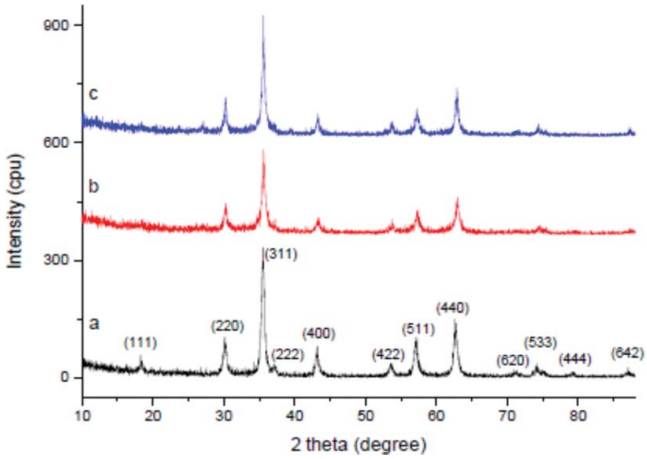

Figure 6. XRD patterns of N-MNP-1(a), N-MNP-2 (b) and N-MNP-3(c).

had cubic spinal structure.[16]N-MNP-3 sample even exhibited minor peaks of standard Fe_3O_4 with corresponding plane indexes (111), (222), (620), (533), (444), (642) and (731) at 18.37, 35.60, 71.31, 74.36, 79.36, 87.21, 90.13 2θ (degrees), respectively. Besides, no additional peaks were observed indicating that there were not any impurities in the samples. These results are in parallel with the literature.[17–18]During the coating steps, both oleic acid and PEG were added into system during synthesis without any washing. XRD analysis of OA-MNP-2 and PEG-MNP-2 were also done to investigate whether this influenced the crystal structure of core nanoparticles (Fig. 7).

In Fig. 7, XRD patterns of PEG-MNP-2 and OA-MNP-2 were compared to N-MNP-3. Major diffraction peaks with corresponding plane indexes (220), (311), (400), (422), (511), (440) and minor peaks with (111), (620), (533), (642), (731) plane indexes of core magnetite were also observed in PEG-MNP- 2 and OA-MNP-2 samples which identify that those samples kept their cubic spinal structure after the coating process.

Fourier transform infrared (FTIR) spectroscopy

Naked MNP, oleic acid coated MNP, PEG coated MNP and folic acid functionalized MNP were characterized with FTIR spectroscopy. FTIR spectrum of N-MNP-3 is given in Fig. 8.

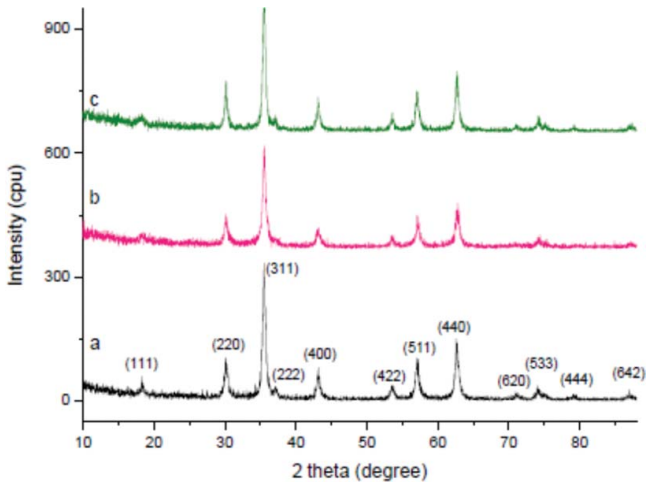

Figure 7. XRD patterns of N-MNP-3(a), OA-MNP-2(b), PEG-MNP-2 (c).

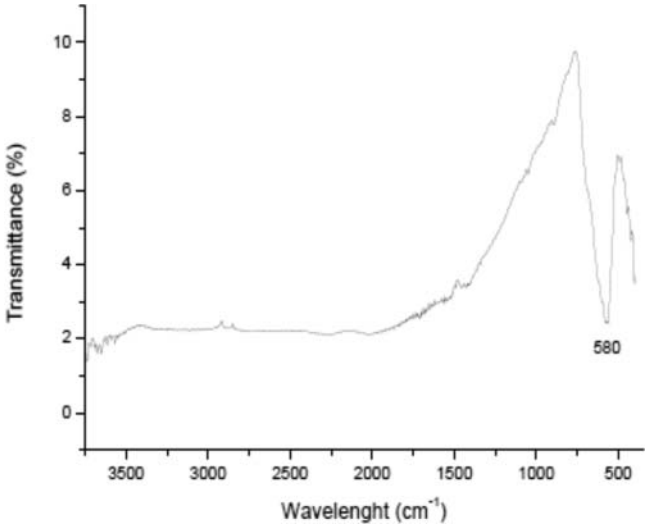

Figure 8. FTIR spectrum of N-MNP-3.

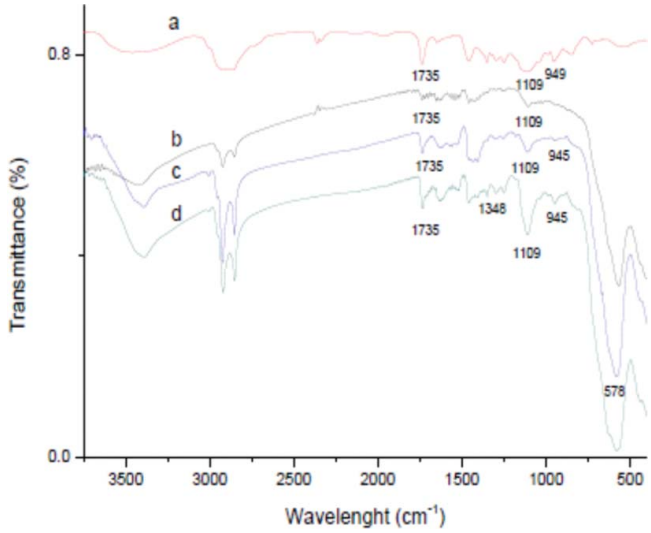

Figure 10. FTIR spectra of Polyethylene glycol monooleate (a), PEG-MNP-1 (b), PEG-MNP-2 (c) and PEG-MNP-3 (d).

The band with the wavelength 580 cm^{-1} belongs to vibrations of the Fe-O bond of magnetite indicating that synthesized N-MNP-3 was magnetite.[12]

FTIR spectra of pure oleic acid and OA-MNP-1 were given in Fig. 9. Pure oleic acid gave strong peaks at 2924 cm^{-1} and 2854 cm^{-1} belonging to asymmetric and symmetric CH_2 stretch, respectively. Peak at 3005 cm^{-1} was attributed to C—H bond in C=C—H. Vibration of C=O stretch exhibited an intense band at 1710 cm^{-1}. Peaks at 1462 cm^{-1} and 937 cm^{-1} were derived from the O–H in-plane and out-of-plane stretch, respectively. The peak appeared at 1285 cm^{-1} exhibited the presence of the C-O stretch.[19–21] OA-MNP-1 sample exhibited broad band around 3500 cm^{-1} corresponding to surface –OH groups. Asymmetric and symmetric CH_2 stretching bands at 2924 cm^{-1} and 2854 cm^{-1} of pure oleic acid, shifted to 2922 cm^{-1} and 2852 cm^{-1} in OA-MNP-1 sample (Fig. 9). A similar shift was also reported in the literature.[12, 22]This shift was attributed to the adsorption of oleic acid onto surface of magnetite nanoparticles.[20,21]The strong peak of C=O stretch at 1710 cm^{-1} shifted to 1636 cm^{-1} and 1541 cm^{-1}.

FTIR spectrum of Polyethylene glycol monooleate, PEG-MNP-1, PEG-MNP-2 and PEG-MNP-3 were given in Fig. 10. Characteristic Fe-O band vibrations of Fe_3O_4 were observed at 578 cm^{-1}. Broad peak around 3500–3250 cm^{-1} were due to –OH groups.[11] Strong bands appeared at 2923 and 2852 cm^{-1} were due to $-CH_2$ stretching while broad band at 1465 cm^{-1} belonged to bending vibrations of $-CH_2$. At 1735 cm^{-1} stretching vibration of the C=O was observed.[23]Symmetric stretching of C-O-C at 1109 cm^{-1} indicating the presence of PEG was clearly seen in the spectra of PEG-MNP-2 and PEG-MNP-3 while a mild peak was observed in PEG-MNP-1. However, peak at 945 cm^{-1} derived from out of plane bending vibrations of the C—H of PEG was observed only in the adsorption spectra of PEG-MNP-2 and PEG-MNP-3.[13, 24] Peak of C-O-C at 1109 cm^{-1} became very sharp in the spectra of PEG-MNP-3. Additionally, the peak at 1348 cm^{-1} derived from asymmetric stretching of C-O-C belonging to the spectra of PEG was also observed in PEG-MNP-3.

Figure 11 shows FTIR spectra of pure folic acid, FA-MNP-1 and FA-MNP-2. Both, FA-MNP-1 and FA-MNP-2 samples revealed parallel peak patterns with pure folic acid. Vibration of NH stretching at 3329 cm^{-1} was seen in both FA-MNP-1 and FA-MNP-2 spectrum, indicating the

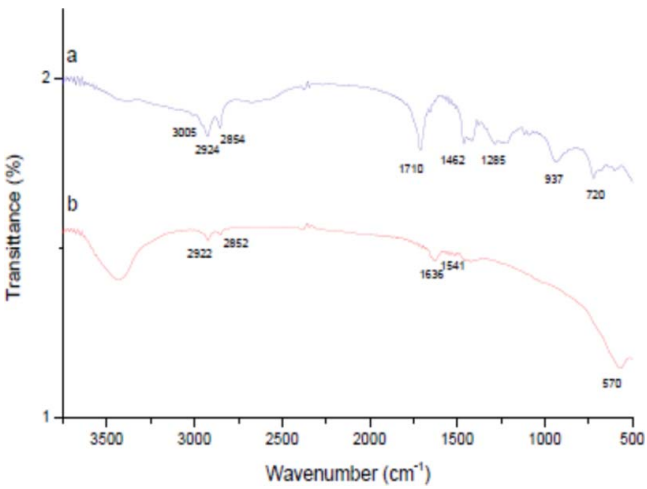

Figure 9. FTIR spectra of pure oleic acid (a) and OA-MNP-1(b).

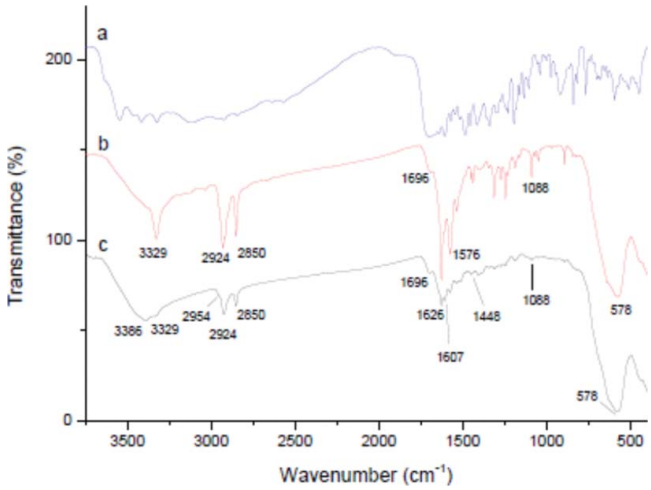

Figure 11. FTIR spectra of pure folic acid (a), FA-MNP-1(b) and FA-MNP-2(c).

presence of folic acid. The peak seen at 3386 cm^{-1} was due to the presence of terminal OH group in PEG[24].Peaks of CH_2 group, seen at 2954, 2924 and 2850 cm^{-1} were corresponded to oleic acid and PEG in both samples. The band at 1696 cm^{-1} was derived from C=O stretching of folic acid and PEG. The intense peak at 1626 cm^{-1} was the characteristic band of folic acid, shifted from 1639 cm^{-1}, corresponding to vibration of C=O. Peaks at 1607 and 1448 cm^{-1} were corresponded to NH_2 bending vibration and phenyl ring of folic acid. Peak at 1088 cm^{-1} indicated C-O-C ether stretching of PEG, while vibration band at 578 was derived from Fe-O stretching of Fe3O4[13,25].

In Fig. 12 different and similar peaks of OA-MNP-2, PEG-MNP-2, FA-MNP-1 and FA-MNP-2 were given. All four curves revealed the characteristic peaks of oleic acid around 2924 cm^{-1}, 2854 cm^{-1} and 3005 cm^{-1} belonging to CH_2 stretching and C—H stretchings. Additionally, Fe-O stretching of Fe_3O_4 was observed around 580 cm^{-1} in the curves of all samples. Important different peaks indicating the presence of PEG or folic acid were indicated with arrow. Compared to OA-MNP-2, additional peaks around 1109 and 945 cm^{-1} were observed in the curve of PEG-MNP-2, FA-MNP-1 and FA-MNP-2 attributed to C-O-C stretching and bending of C—H of PEG. In the adsorption spectrum of FA-MNP-1 and FA-MNP-2, new peaks at 1696 cm^{-1} and 1626 cm^{-1} were derived from mainly folic acid.

Vibrating sample magnetometer (VSM)

Magnetization characteristics of naked, OA coated, PEG coated and FA functionalized MNPs were analyzed by VSM at room temperature (23°C). Since the cell culture experiments were carried out at body temperature, VSM analyses were also performed at 37°C. Magnetization curves of N-MNP-3, OA-MNP-2, PEG-MNP-2, FA-MNP-1 and FA-MNP-2 nanoparticles exhibited very similar curves (Fig. 13). It could be stated that they exhibited magnetic characteristics similar to superparamagnetism. As compared to N-MNP-3, a general decrease has been observed in saturation magnetization values of other nanoparticles. This drop was attiributed to diamagnetic coating

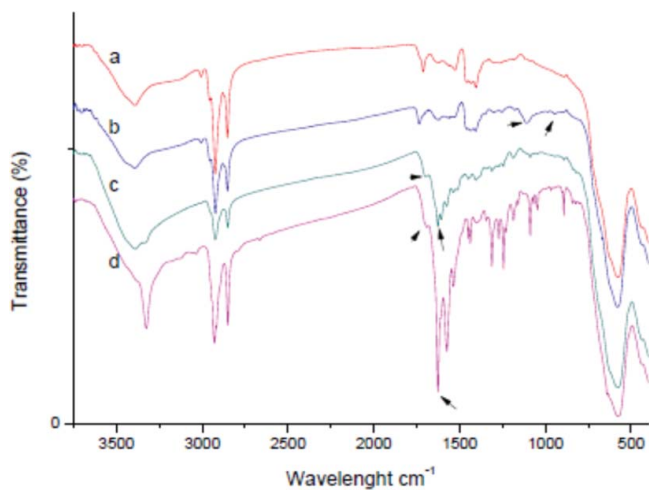

Figure 12. FTIR spectra of OA-MNP-2(a), PEG-MNP-2(b), FA-MNP-1(c) and FA-MNP-2(d).

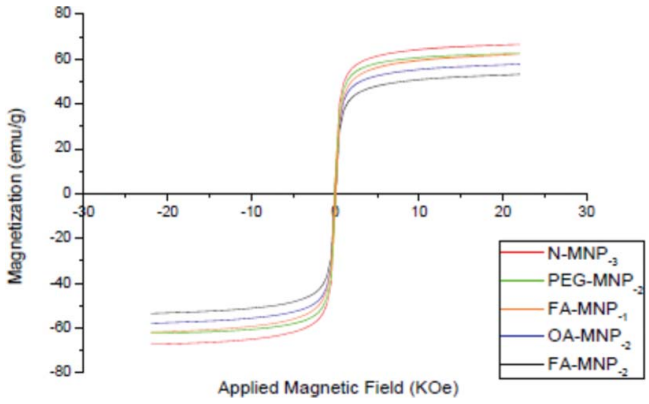

Figure 13. Hysteresis loops of N-MNP-3, OA-MNP-2, PEG-MNP-2, FA- MNP-1 and FA- MNP-2 at 23 °C.

materials on the surface of nanoparticles.[2, 25–27] Oleic acid is a diamagnetic material. Thus, it decreases the Ms value of N-MNP-3 from 66.89 (emu/g) to 57.87 (emu/g) at 23°C. A drop of 13.5% in Ms was recorded. Liu et al. found the Ms values of 58 (emu/g) and 46 (emu/g) for the naked magnetite and oleic acid coated magnetite nanoparticles at room temperature, respectively. They calculated oleic acid layer mass percentage from this data as 20%.

Magnetization behaviors of N-MNP-3, OA-MNP-2, PEG-MNP-2, FA-MNP-1 and FA-MNP-2 were also examined at 37°C comparatively (Fig. 14). A general decrease in Ms values was observed. They exhibited negligible coercivity and remanent magnetization. It could be concluded that, N-MNP-3, OA-MNP-2, PEG-MNP-2, FA-MNP-1 and FA-MNP-2 retain their superparamagnetic characteristics at 37°C.

Superparamagnetic materials do not show any coercivity in magnetization curve. Besides, their hysteresis loops show similar pattern at different temperatures.[28] N-MNP-3 nanoparticles exhibited very similar magnetization curves at 23°C and 37 °C with the Ms values of 66.89 and 59.34 (emu/g), respectively. The slight decrease in Ms by increasing temperature was also stated in the literature. Bean and Jacops studied magnetization of iron nanoparticles which

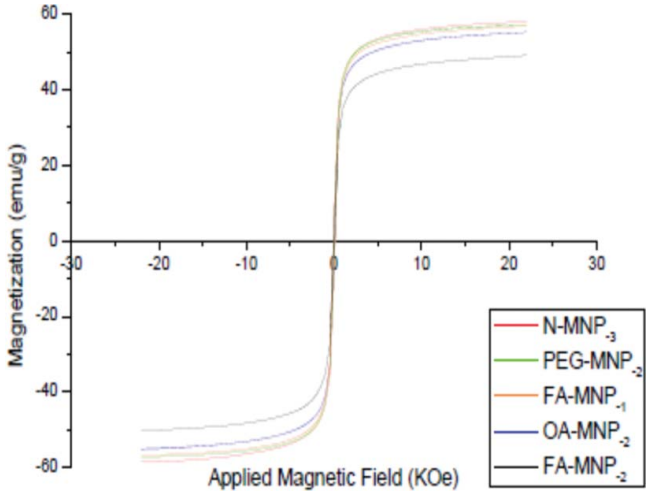

Figure 14. Hysteresis loops of N-MNP-3, OA-MNP-2, PEG-MNP-2, FA-MNP-1 and FA-MNP-2 at 37 °C.

had similar pattern of superparamagnetic magnetization curves at 77 K and 200 K with slightly lower magnetization value at 200 K.[29] This drop of Ms value is explained by the Langevin theory stating that while magnetization is proportional to applied field, it decreases by elevated temperatures.[30] Additionally, 66.89 (emu/g) Ms value of N-MNP-3 agrees with previous studies. Hai et al. found the saturation magnetization as 60 (emu/g) for uncoated Fe_3O_4 nanoparticles which were synthesized by co-precipitation method.[31] Similar to N-MNP-3, each samples OA-MNP-2, PEG-MNP-2, FA-MNP-1 and FA-MNP-2 exhibited similar magnetization curves at 23°C and 37°C.

Cytotoxicity studies of magnetic nanoparticles

Cytotoxicities of naked nanoparticles, oleic acid coated nanoparticles, PEG coated nanoparticles and folic acid conjugated nanoparticles were determined by using XTT assay kit. 10,000 MCF-7 cells/well were seeded to 96 well plates at 37°C. Both drug sensitive and drug resistant (Doxorubicin, Paclitaxel, Zoledronic acid) MCF-7 cells that were exposed to MNPs were incubated for 72 h at 37°C. Cell proliferation profiles were determined by considering control groups.

Cytotoxicity of naked MNP, oleic acid coated MNP, PEG coated MNP and folic acid functionalized MNP on drug sensitive MCF-7 cell line

To understand biocompatibility of naked magnetite nanoparticles or whether they were toxic to MCF-7/S cells, XTT assay was performed. MCF-7 cells incubated with different concentrations of naked magnetic nanoparticles (0 – 500 μg/ml) did not exhibit a dramatic cell death. At 500 μg/ml, significant drop in cell proliferation was observed. Maximum cell death compared to untreated cells observed at 500 μg/ ml was 15%. It could be concluded that N-MNP-3 nanoparticles did not exhibit a significant toxic effect on MCF-7 cells after 72 hr incubation between the concentration range of 0 – 250 μg/ml. Hence, they can be used and fabricated in further studies. Cytotoxicity of oleic acid coated OA-MNP-2 nanoparticles was determined with XTT assay. MCF-7/S breast cancer cells were incubated with OA-MNP-2 in the concentration range of 0 – 500 μg/ ml for 72 hr at 37°C. OA-MNP-2 nanoparticles were found to be biocompatible and not toxic to MCF-7 cells in the concentration range of 0 – 125 μg/ml for 72 hr. A significant decrease in the cell proliferation relative to untreated cells was observed at the nanoparticle concentration of 250 and 500 μg/ ml. Cell proliferation at 250 and 500 μg/ml was 89 and 84%, respectively. OA-MNP-2 could be used for in vitro studies with the concentration of 0–125 μg/ml. Toxicity profile of PEG-MNP-2 nanoparticles suggested that up to 500 μg/ml, significant cell toxicity was not observed. Cell proliferation of 84% was observed at 500 μg/ml. It could be concluded that PEG-MNP-2 revealed toxicity on MCF-7 cells at 500 μg/ml concentration compared to untreated control group. In the concentration range of 0 – 500 μg/ml, FA-MNP-1 nanoparticles did not have significant toxic influence on MCF-7/S cells compared to untreated cells (Fig. 15).

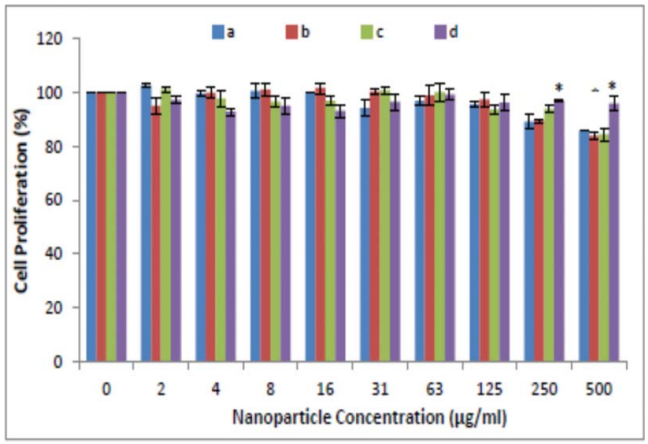

Figure 15. Cell proliferation profile of MCF-7/S breast cancer cells treated with a)N-MNP-3, b) OA-MNP-2, c) PEG-MNP-2 and d) FA-MNP-1 for 72 hr. $^{*}p<0.05$ compared to same concentration of N-MNP-3 nanoparticle treated cells. Results were given as Mean SEM. All experiments were carried out in triplicates.

Cytotoxicity of folic acid functionalized MNP on drug resistant cells

FA-MNP-1 nanoparticles have been also studied to learn their toxicity profile on drug resistant MCF-7 breast cancer cell lines. Fig. 16 demonstrates the cell proliferation profiles of MCF-7/Dox, MCF-7/Pac and MCF-7/Zol cells.

FA-MNP-1 nanoparticles were found to not to have severe toxic effects on MCF-7/Dox cells in the concentration range of 0 – 250 μg/ml. A significant decrease in the cell proliferation relative to untreated cells was observed at the nanoparticle concentration of 500 μg/ml. Cell proliferation at 500 μg/ml was 91%. MCF-7/Pac cells incubated with FA-MNP-1 did not exhibited a significant cell death in the concentration range of 0 – 250 μg/ml. Maximum cell death compared to untreated cells was observed at 500.00 μg/ml and found as 9%. It could be concluded that FA-MNP-1 nanoparticles did not revealed a significant toxic effect on MCF-7/Pac cells after 72 hr incubation in the concentration range of 0 – 250 μg/ml. A significant

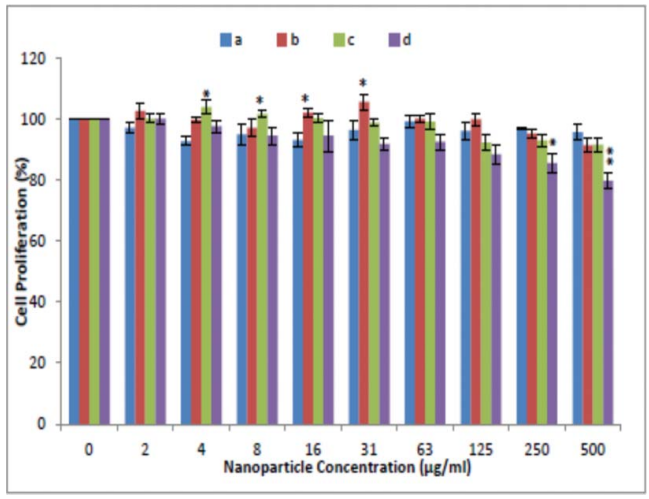

Figure 16. Cell proliferation profile of a)MCF-7/S, b)MCF-7/Dox, c)MCF-7/Pac and d)MCF-7/Zol breast cancer cells treated with FA-MNP-1 for 72 hr. $^{*}p<0.05$ and $^{**}p< 0.01$ compared to same concentration of $Fe_3O_4{}^{*}$ nanoparticle treated cells. Results were given as Mean SEM. All experiments were carried out in triplicates.

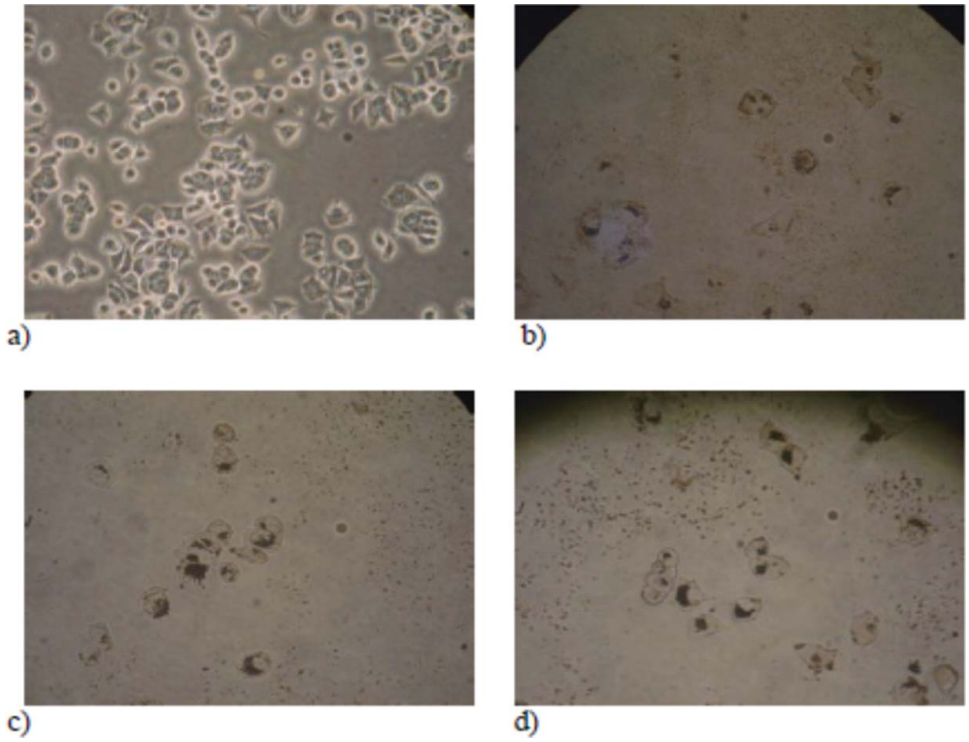

Figure 17. Light microscopy images of a) untreated control MCF-7/S cells, and MCF-7/S cells treated with 500 μg/ml of b) N-MNP-1, c) PEG-MNP-2 and d) FA-MNP-1 for 48 hr (400X magnification).

decrease in the MCF-7/Zol cells proliferation relative to untreated cells was observed at the nanoparticle concentrations of 125, 250 and 500 μg/ml with cell proliferation values of 88%, 85 and 79%, respectively. In general, up to concentrations of 31 and 16 μg/ml, Doxorubicin and Paclitaxel resistant cell lines revealed significant increases in cell proliferation compared to same concentration treated sensitive cells. Increase in the cell proliferation was also reported in the literature.[32,33,34]The rise of cell proliferation in lower concentrations may arise from the absorption of the endocytosed MNP in cell. In the literature, the research of Li et al. indicated that folic acid receptor expression was upregulated in the taxol resistant nasopharyngeal carcinoma cells compared to sensitive nasopharyngeal carcinoma cells.[35]Similarly, Györffy et al. reported upregulation of folic acid receptor expression in Doxorubicin resistant breast cancer tumor cells compared to sensitive ones.[36] If there is an upregulated folic acid receptor expression in our resistant cell lines, this could lead to endocytosis of higher amounts of FA-MNP-1 leading to higher absorption values for resistant cell lines compared to sensitive cells. However, to confirm this, expressional analysis of folic acid receptor in resistant and sensitive cell lines should be performed and cross-checked with nanoparticle uptake studies. In the treatment of higher concentrations of FA-MNP-1, significant decreases in cell viability was observed. Increased levels of FA-MNP-1 endocytosis could prevent cell proliferation.

FA-MNP-1 nanoparticles did not exhibit severe toxicity neither on sensitive nor on resistant cell lines up to 125 μg/ml. Since folic acid conjugated nanoparticles are taken up into cell by folic acid mediated endocytosis, they are also successful in bypassing drug resistance derived from upregulation of efflux pumps like MDR1, MRP1 and BCRP.[37]In previous researches, it was demonstrated that the MCF-7/Dox, MCF-7/Pac and MCF-7/Zol resistant cell lines used in this study overexpressed BCRP, MRP1 and MDR1, significantly.[38]Thus, with the loading of an appropriate drug cargo, it can be used as possible drug delivery systems to resistant cell lines.

Light microscopy images

MCF-7/S cells treated with 500 μg/ml of N-MNP-1, PEG-MNP-2 and FA-MNP-1 for 48 hr were examined under light microscopy. The images of observations were given in Fig. 17. MCF-7/S cells exposed nanoparticles seems to tolerate incubation with particles. Compared with the control, MNP treated cells exhibited lesser proliferation. This observation was in agreement with XTT assay results. All the images were taken after PBS washing step. Thus, it can be argued that, MCF-7/S cells could take up both naked and coated nanoparticles. Fig. 17 demonstrates that endocytosed MNP had a tendency to accumulate around nucleus inside the cell. Similar observations were reported in the literature.[34, 38]

Conclusion

In this study, the synthesized magnetite nanoparticles were found to have appropriate size, surface chemistry, magnetization, non-toxic properties and biocompatibility which are suitable for biomedical applications. Folic acid conjugated PEG covered magnetic nanoparticles were characterized in detail. They have a potential to be used in biomedical studies such as drug delivery, hyperthermia and MRI. Since those particles have a hydrophobic layer covered with hydrophilic PEG

corona, they have a proper design for delivery of lipohilic drugs. Due to their magnetic core these MNPs can be targeted to tumor site in an applied magnetic field. Besides, folic acid on MNP surface could help to receptor mediated endocytosis of nanoparticles and by this way drug resistance obstacle in chemotherapy could be prevented. To illustrate these effects further studies are needed.

References

[1] Albuquerque, M. L. S.; Gluedes, I.; Alcantara, P.; Moreira, S. G. C. Infrared absorption spectra of Buritti oil. *Vib. Spectrosc.*. **2003**, *33*, 127–131.

[2] Ankamwar, B.; Lai, T. C.; Huang, J. H.; Hsia, M.; Chen, C. H.; Hwu, Y. K. Biocompatibility of Fe3O4 Nanoparticles Evaluated by in vitro Cytotoxicity Assays Using Normal, Glia and Breast Cancer Cells. *Nanotechnology*. **2007**, *21*, 075102.

[3] Arias, J. S.; Ruiz, A.; Gallardo, V.; Delgado, A. V. Tegafur loading and release properties of magnetite / poly (alkylcyanoacrylate) (core/shell) nanoparticles. *J. Control Release.* **2007**, *125*, 50–8.

[4] Bean, J. P.; Jacops, I. S. Magnetic granulometry and super-paramagnetism. *J. Appl. Phys.*. **1956**, *27*, 1448.

[5] Boyer, C.; Whittaker, M.; Bulmus, V.; Jingquan, L.; Davis, T. The design and utility of polymer-stabilized iron oxide nanoparticles for nanomedicine applications. *NPG Asia Mater.*. **2010**, *2* (1), 23–30.

[6] Byrne, J. D.; Betancourt, T.; Peppas, L. B. Active targeting schemes for nanoparticle systems in cancer therapeutics. *Adv. Drug Deliv. Rev.* **2008**, *60*, 1615–1626.

[7] Caruntu, D.; Caruntu, G.; Chen, Y.; O'Connor, C. J.; Goloverda, G.; Kolesnichenko, V. L. Synthesis of variable-size nanocrystals of Fe3O4 with high surface reactivity. *Chem. Mater.*. **2004**, *16*, 5527–5534

[8] Cho, K.; Wang, X.; Nie, S.; Chen, Z. G.; Shin, D. M. Therapeutic Nanoparticles for Drug Delivery in Cancer. *Clin. Cancer Res.* **2008**, *14*, 1310–1316.

[9] Demirel, K. M.; Darcansoy, I. O.; Ural, A. U.; Gündüz, U. In Vitro Evaluation of Zoledronic Acid Resistance Developed in MCF-7 Cells. *Anticancer Res.* **2007**, *27*, 4031–4037.

[10] Finger, L. W.; Hazen, R. M.; Hofmeister, A. M. High-Pressure crystal chemistry of spinel (MgAl2O4) and magnetite (Fe_3O_4): Comparisons with silicate spinels. *Phys. Chem. Minerals* **1986**, *13*, 215–220.

[11] Gang, J.; Park, S. B.; Hyung, W.; Choi, E. H.; Wen, J.; Kim, H. S.; Shul, Y. G.; Haam, S.; Song, S. Y. Magnetic poly ε-caprolactone nanoparticles containing Fe_3O_4 and gemcitabine enhance anti-tumor effect in pancreatic cancer xenograft mouse model. *J. Drug Target.* **2007**, *15*, 445–453.

[12] Gupta, A. K.; Gupta, M. Synthesis and surface engineering of iron oxide nanoparticles for biomedical applications. *Biomater.* **2005**, *26*, 3995–4021.

[13] Gupta, A. K.; Wells, S. Surface-Modified Superparamagnetic Nanoparticles for Drug Delivery: Preparation, Characterization, and Cytotoxicity Studies. *IEEE Trans Nanobioscience* **2004**, *3*, 66–73.

[14] Györffy, B.; Serra, V.; Jürchott, K.; Abdul-Ghani, R.; Garber, M.; Stein, U.; Petersen, I.; Lage, H.; Diete, M.; Schäfer, R. Prediction of doxorubicin sensitivity in breast tumors based on gene expression profiles of drug-resistant cell lines correlates with patient survival. *Oncogene* **2005**, *24*, 7542–7551.

[15] Hai, N. H.; Luong, N. H.; Chau, N.; Tai, N. Q. Preparation of magnetic nanoparticles embedded in polystyrene microspheres. *J. Phys.: Conf. Ser.* **2009**, *187*, 012009.

[16] Khodadust, R.; Unsoy, G.; Yalcın, S.; Gunduz, G.; Gunduz, U. PAMAM dendrimer-coated iron oxide nanoparticles:synthesis and characterization of different generations. *J. Nanopart. Res.* **2014**, *15*, 1488–1501.

[17] Lan, Q.; Liu, C.; Yang, F.; Liu, S.; Xu, J.; Sun, D. Synthesis of bilayer oleic acid coated Fe_3O_4 nanoparticles and their application in pH-responsive Pickering emulsions. *J. Colloid Interface Sci.* **2007**, *310*, 260–269.

[18] Li, W.; Tan, G.; Ma, Y.; Li, H.; He, G. Inhibition of α folate receptor resulting in a reversal of taxol resistance in nasopharyngeal carcinoma. *Otolaryngol. Head Neck Surg.* **2011**, *20*, 1–9.

[19] Li, X. W.; Lin, X. H.; Zheng, L. Q.; Yu, L. L. Z.; Zhang, Q. Q.; Liu, W. C. Effect of poly (ethylene glycol) stearate on the phase behavior of monocaprate/ Tween80/ water system and characterization of poly (ethylene glycol) stearete modified solid lipid nanoparticles. *Colloids Surf. A Physicochem. Eng. Asp.* **2008**, *317*, 3522–359.

[20] Liu, X.; Kaminski, M.; Guan, Y.; Chen, H.; Liu, H.; Rosengart, A. J. Preparation and characterization of hydrophobic superparamagnetic magnetite gel. *J. Magn. Magn. Mater.* **2006**, *306*, 248–253.

[21] Lu, Y.; Low, P. S. Folate-Mediated Delivery of Macromolecular Anticancer Therapeutic Agents. *Adv. Drug Deliv. Rev.* **2002**, *54*, 675–693

[22] McBain, S. C.; Yiu, H. H. P.; Dobson, J. Magnetic Nanoparticles for Gene and Drug Delivery. *Int. J. Nanomedicine* **2008**, *3*, 169–180.

[23] Mohapatra, S.; Mallick, S. K.; Maiti, T. K.; Ghosh, T. K.; Pramanik, P. Synthesis of highly stable folic acid conjugated magnetite nanoparticles for targeting cancer cells. *Nanotechnology* **2007**, *18*, 385102.

[24] Okassa, L. N.; Marchais, H.; Douziech-Eyrolles, L.; Herve, K.; Cohen-Jonathen, S.; Munnier, E.; Souce, M.; Linassier, C.; Dubois, P.; Chourpa, I. Optimization of Iron Oxide Nanoparticles Encapsulation within Poly(d,l-lactide-co-glycolide) Sub-micron Particles. *Eur. J. Pharm. Biopharm.* **2007**, *67*, 31–38.

[25] Peer, D.; Karp, J. M.; Hong, S.; Farokhzad, O. C.; Margalit, R.; Langer, R. Nanocarriers as an emerging platform for cancer therapy. *Nat. Nanotechnol.* **2007**, *2*, 751–760.

[26] Sonvico, F.; Mornet, S.; Vasseur, S.; Dubernet, C.; Jaillard, D.; Degrouard, J.; Hoebeke, J.; Duguet, E.; Colombo, P.; Couvreur, P. Folate-Conjugated Iron Oxide Nanoparticles for Solid Tumor Targeting as Potential Specific Magnetic Hyperthermia Mediators: Synthesis, Physicochemical Characterization and in Vitro Experiments. *Bioconjug. Chem.* **2005**, *16*, 1181–1188.

[27] Spaldin, N. A. Materials science. Fundamental size limits in ferroelectricity. *Science* **2004**, *304*, 1606–7.

[28] Sun, C.; Lee, J. S. H.; Zhang, M. Magnetic Nanoparticles in MR Imaging and Drug Delivery. *Adv. Drug Deliv. Rev.* **2008**, *60*, 1252–1265.

[29] Sun, J.; Shaobing, Z.; Hou, P.; Yang, Y.; Weng, J.; Li, X.; Li, M. Synthesis and characterization of biocompatible Fe_3O_4 nanoparticles. *J. Biomed. Mater. Res.* **2006**, *80*, 333–341.

[30] Unsoy, G.; Yalcin, S.; Khodadust, R.; Gunduz, G.; Gunduz, U. Synthesis optimization and characterization of chitosancoated iron oxide nanoparticles produced for biomedical applications. *J. Nanopart. Res.* **2012**, *14*, 964–977.

[31] Varadan, V. K.; Chen, L. F.; Xie, J. *Nanomedicine: Design and Applications of Magnetic Nanomaterials, Nanosensors and Nanosystems*. West Sussex: John Wiley & Sons. **2008**, ISBN: 978-0-470-03351-7.

[32] Wu, N.; Lei, F.; Su, M.; Aslam, M.; Wong, K. C.; Dravid, V. P. Interaction of Fatty Acid Monolayers with Cobalth Nanoparticles. *Nano. Lett.* **2004**, *4*, 383–386.

[33] Xiong, F.; Li, J.; Wang, H.; Chen, Y.; Cheng, Y.; Zhu, J. Synthesis, properties and application of a novel series of one-ended monooleate-modified poly (ethylene glycol) with active carboxylic terminal. *Polymer* **2006**, *47*, 6636–6641.

[34] Yallapu, M. M.; Foy, S. P.; Jain, T. K.; Labhasetwaar, V. PEG-functionalized Magnetic Nanoparticles for Drug Delivery and Magnetic Resonance Imaging Applications. *Pharm. Res.* **2010**, *27*, 2283–2295.

[35] Yan, F.; Li, J.; Zhang, J.; Liu, F.; Yang, W. Preparation of Fe3O4/polystyrene composite particles from monolayer oleic acid modified Fe3O4 nanoparticles via miniemulsion polymerization. *J. Nanopart. Res.* **2009**, *11*, 289–296.

[36] Zhang, J.; Rana, S.; Sriavastava, R. S.; Misra, R. D. K. On the chemical synthesis and drug delivery response of folate receptor-activated, polyethylene glycol-functionalized magnetite nanoparticles. *Acta Biomater.* **2008**, *4*, 40–48.

[37] Zhang, L.; He, R.; Gu, H. C. Oleic acid coating on the monodispere magnetite nanoparticles. *Appl. Surf. Sci.* **2006**, *2531*, 2611–2617.

[38] Zhang, Y.; Kohler, N.; Zhang, M. Q. Surface Modification of Superparamagnetic Magnetite Nanoparticles and Their Intracellular Uptake. *Bacteriol.* **2002**, *23*, 1553–1561.